

Study of Nb₃Sn Cable Stability at Self-field Using a SC Transformer

E. Barzi, N. Andreev, V. V. Kashikhin, D. Turrioni, A. V. Zlobin

Abstract— A superconducting current transformer with a maximum DC current of 28 kA has been used for Nb₃Sn cable testing at self-fields under various experimental conditions. A fast data acquisition system was developed and used for accurate measurements of the secondary current. Test results are shown for thirty cables made of MJR, RRP and PIT strands, along with a description of the SC transformer, sample preparation and test procedure. It was found that premature quenches at currents significantly lower than the expected critical currents at low fields were due to electromagnetic instabilities in the superconductor.

Index Terms — Instability, Nb₃Sn, Rutherford cable, Superconducting transformer.

I. INTRODUCTION

TEST results of Nb₃Sn dipole models fabricated at Fermilab have shown that most of the quenches at low currents occurred in the low field regions [1]. The analysis of this phenomenon [2], [3] as well as measurements performed on Nb₃Sn strands used in magnets [4], pointed at large magnetic instabilities in Nb₃Sn strands with high critical current density, J_c , and large effective filament size, d_{eff} . To investigate cable instability, a superconducting (SC) transformer was designed to test cables at low fields using the existing Fermilab's Short Sample Test Facility and strand power supply. This transformer, which was designed to provide a maximum current in its secondary winding close to 28 kA, proved to be an inexpensive way to a fast turn-around and reliable data, as typical short sample limits for Fermilab's Nb₃Sn coils are larger than 20 kA and approach 28 kA in some designs. The transformer is being extensively used to test impregnated and non-impregnated cables, enabling investigation of the various effects that have been tied to cable instability, such as d_{eff} , matrix RRR and cable cooling conditions. This paper describes the experimental setup and the results obtained in a systematic run of thirty cable tests, including impregnated and non-impregnated 28x1 mm rectangular and keystone Powder-in-Tube (PIT) cables, 28x1 mm keystone Modified Jelly Roll (MJR), and 39x0.7 mm rectangular and keystone Restacked Rod Process (RRP) cables of various packing factors.

Manuscript received October 5, 2004. This work was supported by the U.S. Department of Energy.

All authors are with the Fermi National Accelerator Laboratory, Batavia, IL 60510 USA (corresponding author: 630-840-3446; fax: 630-840-2383; e-mail: barzi@fnal.gov).

II. EXPERIMENTAL PROCEDURE

A. SC Transformer Parameters

To measure transport current capability of cables at low fields, a SC transformer that was originally designed to study Nb₃Sn cable splicing techniques [5] was modified and used. Two changes were implemented. The secondary winding was modified to accommodate a straight cable sample of about three pitch lengths. To increase the maximum secondary current, a new primary coil with a larger number of turns, N1, was fabricated. It was wound out of 112 turns over 6 layers on a G-10 core using 0.8-mm NbTi strand (SSC inner layer strand) coated with 50- μ m polyimide insulation.

The new shape of the transformer secondary circuit and the schematic of the primary and secondary windings with voltage taps and instrumentation are shown in Fig. 1. Only the section made of 27 x 1 mm NbTi strands is shown on the picture in Figure. A spot heater used to quench the secondary coil can be seen on the left bend, and a Rogowski coil to measure the secondary current is shown close to the right bend. The Nb₃Sn cable sample is placed in the straight groove of the G-10 structure and spliced to the NbTi cable ends. The transformer secondary winding is equipped with six pairs of voltage taps to monitor quench location. The voltage taps cover the whole length of the secondary loop, as shown in Figure (lower half). The six voltage signals, the integrated Rogowski signal (proportional to the secondary current) and the primary current from the analog output of the power supply were acquired with a NI DAQ card at 25 kHz rate.

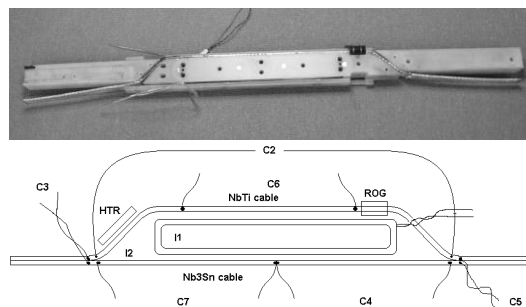


Fig. 1. G-10 structure with groove showing the shape of the transformer secondary winding (top). Only the NbTi cable is shown in the groove. Lower half of Figure shows schematic of primary and secondary windings with voltage taps and instrumentation.

The maximum transfer function, calculated for the primary winding using OPERA, is $B1_{max}/N1/I1 = 0.0497$ T/kA for $I2=0$. The intersection of the primary load line associated to $B1_{max}$ with the SSC strand critical surface occurs at ~ 750 A, consistently with the maximum currents typically obtained in the primary with $I2=0$. The transfer function of the secondary winding was calculated to be $B2_{max}/I2 = 0.0588$ T/kA for $I1=0$. The intersection of the secondary load line associated to $B2_{max}$ with the NbTi cable critical surface occurs at about 35 kA.

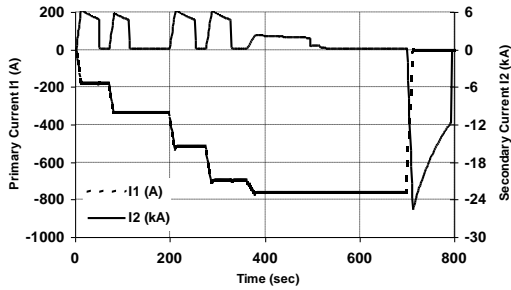


Fig. 2. Typical transformer excitation diagram.

A typical current excitation diagram is shown in Fig. 2. When the maximum current is attained in the primary and the secondary current is brought to zero, the primary coil is ramped down at various ramp rates, ranging from 10 to about 200 A/s. The higher the ramp rate and the lower the splice resistance in the secondary loop, the larger the current obtained in the secondary, as the time for the secondary current to decay is shorter. A maximum primary current of ~ 750 A can be reached in the upgraded transformer, leading to maximum secondary currents close to 28 kA with typical splice resistances of 1 to 1.5 nOhm. Current imbalances between strands were analyzed and found negligible [6].

The calculated quench current of a MJR cable made of 28 x 1 mm strands [3] and some load lines of a Nb₃Sn sample in the transformer secondary winding are shown in Fig. 3. This plot shows that testing with the SC transformer allows measuring minimum cable quench currents in the low field region (< 2 T).

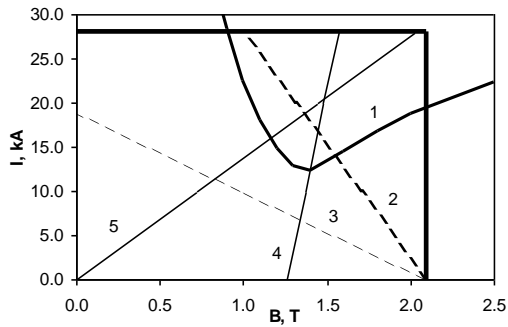


Fig. 3. Calculated quench current (1) of a MJR cable [3], and some load lines (2-5) of the transformer secondary winding.

TABLE I
STRAND PARAMETERS

Strand Parameter	PIT	MJR1	MJR2	RRP
Diameter, mm	1.00	1.00	1.00	0.70
d_{eff} , μ m	~ 50	~ 110	~ 110	~ 80
Cu, %	53.6	47.8	46.7	50.0
Twist pitch, mm/turn	20	23	23	12

TABLE II
PARAMETERS OF CABLE SAMPLES

Sample No.	Strand type	Strand size, mm	No. of strands	HT	Impreg-nation	RRR	$I_{c,ex}(12T,4.2K)$, A
1,2	PIT	1.0	28	A	Y	~ 90	590
3	PIT	1.0	28	B	N	~ 80	600
4,5	MJR1	1.0	28	C	Y	~ 5	700
6,7	MJR2	1.0	28	C	N	~ 5	780
8	MJR2	1.0	28	D	N	~ 50	$\sim 800^a$
8a ^b ,9,10	MJR2	1.0	28	D	Y	~ 50	$\sim 800^a$
11-16	RRP	0.7	39	E	Y	~ 5	$\sim 480^a$
17-20	RRP	0.7	39	E	N	~ 5	$\sim 480^a$
21,22	RRP	0.7	39	F	Y	~ 7	470
23-26	RRP	0.7	39	F	N	~ 7	470
27,28	RRP	0.7	39	G	Y	~ 12	430
29,30	RRP	0.7	39	G	N	~ 12	430

^aEstimated based on round strand data.

^bSample 8a is sample 8 impregnated after testing.

TABLE III
CABLE HEAT TREATMENT CYCLES

Heat Treatment		Step 1	Step 2	Step 3
A	SML_NOM	Ramp rate, °C/h	25	
		Temperature, °C	655	
		Duration, h	170	
B	SML_MOD	Ramp rate, °C/h	25	
		Temperature, °C	675	
		Duration, h	100	
C	OST_NOM	Ramp rate, °C/h	25	50
		Temperature, °C	210	340
		Duration, h	100	48
D	OST_SHORT	Ramp rate, °C/h	25	50
		Temperature, °C	210	340
		Duration, h	100	48
E	HT-1	Ramp rate, °C/h	25	50
		Temperature, °C	210	400
		Duration, h	48	48
F	HT-2	Ramp rate, °C/h	25	50
		Temperature, °C	210	400
		Duration, h	48	48
G	HT-3	Ramp rate, °C/h	25	50
		Temperature, °C	210	400
		Duration, h	48	48

B. Strand and Cable Description

Two slightly different multifilamentary MJR Nb₃Sn strands and an RRP strand by Oxford Superconducting Technology (OST), and a PIT Nb₃Sn strand by ShapeMetal Innovation (SMI), were used to manufacture the cable samples. The strands parameters are summarized in Table I.

The parameters of the thirty cable samples that were tested are shown in Table II. The PIT and MJR2 cables were fabricated at FNAL, whereas the MJR1 and RRP cables were fabricated at LBNL. All cables had the same pitch length of

Formatted

about 110 mm and packing factors within 88.4% to 90.0%. Approximately half of the cables had rectangular cross section and half were keystoneed with a keystone angle of 0.9 ± 0.1 degrees. No correlation of the results with cross section type or packing factor was found.

C. Sample Preparation

The Nb₃Sn cable samples were heat treated in Argon inside SS holders. The heat treatment (HT) cycles used are shown in Table III. Samples were insulated with ceramic insulation and binder. About half of the cables were impregnated using a CTD impregnation procedure after sandwiching the cable sample between two 1 mm thick G-10 strips.

III. RESULTS AND DISCUSSION

All tests were performed at 4.2 K and for some samples also at 2.8 K. Typical quench sequences are shown in Fig. 4 for cables of various Nb₃Sn technologies, including results of a test run performed with the transformer on a MJR cable (Sample 4), which was compared with results of identical cables tested at self-field at BNL (also shown in Fig. 4) and at CERN [7]. The average quench currents measured at FNAL (14,644 A), at BNL (15,241 A), and at CERN (16,450 A) are in good agreement.

Test results of all cables are summarized in Table IV, including for each sample the mean quench current I_q , its standard deviation σ_{I_q} and the number of quenches. Some samples had a short training. Quench current variation at the plateau was $\sim 4\%$ ~~less than~~ ~~42%~~, but the I_q variation between similar samples was sometimes as large as ~~quite large~~ ~~625%~~.

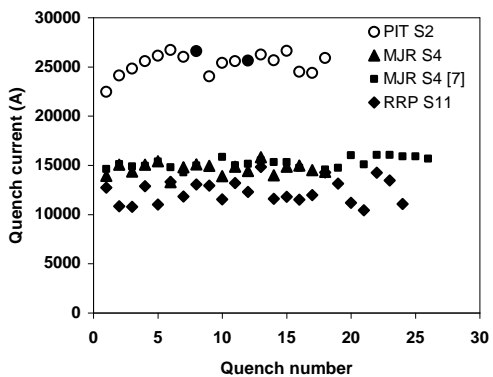


Fig. 4. Examples of cable sample test results. Test results for sample 4 (made of 28 x 1 mm MJR strands) are compared with test results performed at self-field on an identical cable at BNL [7]. For PIT sample 2, open circles show maximum current without quench and the solid circles represent quenches.

A. Effect of Sample Impregnation and Test Temperature

Impregnation improves cable mechanical stability, but degrades strand cooling conditions, and can also be source of additional thermal disturbances due to epoxy cracking. Both impregnated and non-impregnated samples were tested to study this effect. Results on impregnated cables were compared with

magnet test data, and non-impregnated cables tests were compared with strand tests, as strands are in contact with LHe. In this latter case, the best correlation for the I_q 's was obtained when performing the voltage-field (V-H) procedure at constant transport current [4].

TABLE IV
SUMMARY OF CABLE TEST RESULTS

Sample No.	T=4.2 K			T=2.8 K		
	Average ^a I_q , A	σ_{I_q} , A	No. of quenches ^b	Average ^a I_q , A	σ_{I_q} , A	No. of quenches ^b
1	23332	-	0			
2	26114	688	2			
3	27374	-	1	27759	-	0
4	14644	617	18			
5	10194	432	21			
6	18715	788	13	19745	658	11
7	18218	746	13	18981	803	10
8	27539	-	0			
8a	21029	771	16			
9	25501	755	8			
10	26609	501	4			
11	12326	1217	24			
12	15769	719	17			
13	15249	714	23			
14	12502	310	17			
15	15391	889	19			
16	15782	634	17			
17	16373	914	19			
18	13793	746	19			
19	17385	904	17			
20	13493	719	19			
21	17004	885	11	18268	543	11
22	18533	911	12	20500	867	9
23	18350	756	17	19029	684	11
24	17195	929	18			
25	19599	618	11	20151	732	10
26	18965	498	11	19723	794	10
27	21278	629	12	22846	523	4
28	20573	832	11	21194	829	10
29	20489	1069	12	21737	426	5
30	21736	657	12	22577	639	5

^aQuench current was averaged over the number of quenches shown in Table.
^bWhen the sample never quenched, No of quenches = 0 and the maximum current reached by the sample is shown in the Average I_q column.

TABLE V
EFFECT OF CABLE IMPREGNATION AT 4.2 K

Sample No.	HT	Impregnation	Average ^a I_q , A	I_q , N/ I_q , Y
2	A	Y	26114	
3	B	N	27374	1.05
4,5	C	Y	12419	1.49
6,7	C	N	18467	
8	D	N	>27539	
8a,9,10	D	Y	23104	>1.19
11-16	E	Y	14503	
17-20	E	N	15261	1.05
21,22	F	Y	17769	
23-26	F	N	18527	1.04
27,28	G	Y	20926	
29,30	G	N	21113	1.01

^aQuench current was averaged over average I_q 's of samples in first column.

Formatted
Formatted
Formatted

The impregnation effect, shown in Table V as the ratio of the average I_q at 4.2 K of the non-impregnated cables to that of the impregnated ones, is generally small, which is consistent with the assumption of adiabatic flux jumps. The effect seems to be larger for samples 4 to 7, which may be due to the difference in J_c between these samples (see Table II). The impregnation effect at 2.8 K, when measured for the same sets of cables, was smaller than at 4.2 K.

Changing test temperature from 4.2 K to 2.8 K varies the material thermal capacity C_p by a factor of 3.5, and the cable cooling conditions are also different. The temperature effect, shown in Table VI as the ratio of the average I_q of a cable at 2.8 K to that at 4.2 K, is small and on the order of 1.05 ± 0.03 .

TABLE VI
EFFECT OF TEMPERATURE

Sample No.	Average ^a I_q , A		$I_q(2.8K)/I_q(4.2K)$
	4.2 K	2.8 K	
3	27374	27759	1.01
6	18715	19745	1.06
7	18218	18981	1.04
21	17004	18268	1.07
22	18533	20500	1.11
23	18350	19029	1.04
25	19599	20151	1.03
26	18965	19723	1.04
27	21278	22846	1.07
28	20573	21194	1.03
29	20489	21737	1.06
30	21736	22577	1.04

^aAverage current over the number of quenches shown in Table IV.

B. Comparison with Instability Model

According to [3], J_c and d_{eff} are two main parameters that account for electromagnetic instabilities in a superconductor. Table VII shows the ratio of $I_q(B_{self-field})$ to $I_c(B_{self-field})$, calculated using measured values of the $I_c(12T, 4.2K)$ of extracted strands (as shown in the last column of Table II) and Summers parameterization [8]. It can be observed that at low fields (1-2 T) magnetic instabilities reduce the cables quench currents to only 5-15% of their critical value. The data are consistent with calculations [3] for the MJR and the RRP. For the PIT, there is a difference of a factor of 2, which has yet to be understood.

TABLE VII
NORMALIZED CABLE QUENCH CURRENT IN SELF-FIELD

Cable	$I_q(B_{self-field})/I_c(B_{self-field}) @ 4.2 K$	
	measurement	calculation
PIT	0.14-0.15	0.38
MJR	0.06-0.12	0.05
RRP	0.07-0.14	0.15

C. Effect of RRR

The effect of RRR on the average cable I_q for the tested Nb₃Sn strand technologies, characterized by a d_{eff} larger than 50 μm, is summarized in Fig. 5. The data point density is higher in the low RRR region where I_q sensitivity to RRR is the largest. It was found that the cable I_q 's for the PIT and MJR, whose strand d_{eff} 's differ by a factor of ~2, were very close in the case of larger RRR. On the other hand, the I_q 's of the RRP

cables, whose strands had a smaller d_{eff} but higher J_c than the MJR, were higher than for the MJR over the tested RRR range. Even if it is true that the RRR improves the absolute I_q value by a factor of 2-2.5, this effect is still only 5-10% relative to the expected critical currents in the low field region.

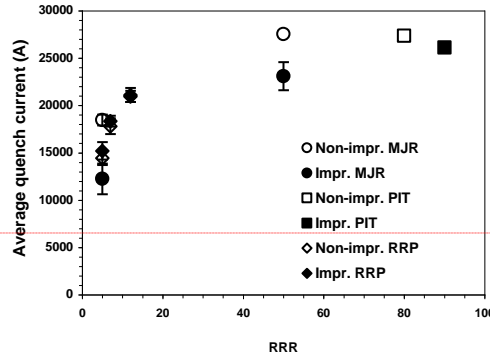


Fig. 5. Effect of RRR on the average I_q 's for impregnated and non-impregnated MJR, PIT and RRP cables at 4.2 K. Error bars show mean deviations. For the non-impregnated MJR with RRR=50, I_{max} is shown.

IV. CONCLUSION

Cable tests at self-field using a SC transformer have allowed gathering fast substantial insight on the effect of the various parameters usually tied to cable instability. It was confirmed that for all tested Nb₃Sn strand technologies, magnetic instabilities cause significant reduction of current carrying capability at low fields, as predicted by instability calculations for these strands. These results are in good agreement with magnet test data as well as with experimental studies of similar strands and cables. These measurements allowed studying effects such as sample cooling conditions, helium temperature and RRR, which are not included in the present model. But in a very few instances, it was found that these effects are relatively small and within 20%. However, the increase of the absolute value of the cable I_q with RRR could be used to improve the instability threshold of unstable high J_c strands and cables used in magnets.

REFERENCES

- [1] S. Feher et al., "Test results of shell-type Nb₃Sn dipole coils", *IEEE Trans. Appl. Sup.*, Vol. 14, No. 2, June 2004, p.349.
- [2] V.V. Kashikhin, A.V. Zlobin, "Magnetic instabilities in Nb₃Sn strands," Fermilab Technical Note, TD-03-032, July 21, 2003.
- [3] V.V. Kashikhin, A.V. Zlobin, "Magnetic instabilities in Nb₃Sn strands and cables," *this conference 5LB02*.
- [4] E. Barzi et al., "Instabilities in transport current measurements of Nb₃Sn Strands," *this conference 2MB04*.
- [5] N. Andreev et al., "Superconducting current transformer for testing Nb₃Sn cable splicing technique", *IEEE Trans. Appl. Sup.*, Vol. 13, No. 2, June 2003, p. 1274.
- [6] J. McDonald et al., "Fast algorithm for computing inductive voltages in a network model of a Rutherford cable", *this conference 5LB05*.
- [7] G. Ambrosio et al., "Critical current and instability threshold measurement of Nb₃Sn cables for high field accelerator magnets," *this conference 2LR03*.

Formatted

Formatted

Formatted

Formatted

Formatted

Formatted

Formatted

- [8] L.T. Summers et al., "A model for the prediction of Nb₃Sn critical current as a function of field, temperature, strain, and radiation damage", *IEEE Trans. Magn.*, Vol. 27, No. 2, March 1991, p. 2041.